Electron Tunnel Sensor Technology

T.W. Kenny, S.B. Waltman, J.K. Reynolds and W.J. Kaiser

Center for Space Microelectronics Technology

Jet Propulsion Laboratory

California Institute of Technology

Pasadena, CA 91109

Abstract

We have designed and constructed a novel electron tunnel sensor which takes advantage of the mechanical properties of micro-machined silicon. For the first time, electrostatic forces are used to control the tunnel electrode separation, thereby avoiding the thermal drift and noise problems associated with piezoelectric actuators. The entire structure is composed of micro-machined silicon single crystals, including a folded cantilever spring and a tip. The application of this sensor to the development of a sensitive accelerometer is described.

Devices used in the measurements of many physical quantities (position, motion, pressure, radiation, temperature) rely on conversion of the physical quantity to a change in the relative separation between a pair of components. Changes in relative position are then detected through changes in the capacitance between the two elements,[1-3] through optical techniques,[4,5] or through flexing of piezoresistors.[6] In each case, large structures are often required to achieve sensitivities that are not limited by readout noise in the transducer. The availability of a more sensitive transducer would, in many cases, allow the construction of sensors with greater sensitivity, smaller mass, smaller volume, less power consumption, or greater bandwidth.

Recently, electron tunneling through a narrow vacuum barrier has been employed as a technique, Scanning Tunneling Microscopy (STM), for imaging the atomic scale structure of surfaces.[7] The tunneling current, I, has the following dependence on the separation between a pair of metallic electrodes, s :

$$I \propto V \exp(-\alpha \sqrt{\Phi}\, s), \qquad (1)$$

where Φ is the height of the tunneling barrier, V is the bias voltage, V is small compared to Φ, and $\alpha = 1.025\ (\text{Å}^{-1}\ \text{eV}^{-1/2})$.[7] For typical values of Φ and s, the current varies by an order of magnitude for each 1 Å change in electrode separation. This sensitivity to relative position is superior to that available in other compact transducers. Since tunneling only occurs in regions where the tip is within several Å of the surface, the active area of the sensor is microscopic. A position sensor based on electron tunneling has already been incorporated into the design for an accelerometer,[8] and several other applications are being considered.

Stable electron tunneling requires control of the separation of the tunnel electrodes to a small fraction of an Angstrom. An analog feedback circuit is used to compare the measured tunnel current to a set-point. The feedback circuit adjusts the voltage applied to an electromechanical actuator to correct for discrepancies between the measured tunnel current and the set-point. The bandwidth of the feedback circuit is limited to less than the resonant frequency of the actuator in order to avoid instability.

Typical vacuum tunneling devices rely upon piezoelectric electromechanical actuators. These actuators suffer from sensitivity to thermal drifts, hysteresis,and creep in the response of the piezoelectric materials; these effects impose severe limitations on the performance of existing tunnel devices. Also, efforts to miniaturize sensors which incorporate piezoelectrics are made difficult by the variety of different materials required for the construction of the device.

There have been recent advances in the sophistication of micro-machining of silicon through the use of anisotropic etchants as well as doping to control etching.[9] These advances have lead to the development of a new class of sensors composed entirely of micro-machined silicon. There are several advantages to the development of sensor components in silicon. First, the well-developed techniques of photo-lithography may be used to control the structure of compact sensor components on the μm-scale. Also, silicon offers extremely high tensile strength combined with relatively low density. Further, silicon single crystal structures show highly reproducible characteristics. Finally, micro-machined silicon sensors are mass-produced inexpensively, and are easily miniaturized or modified to meet the requirements of a particular application.

We have designed and constructed an electron tunnel sensor composed of micro-machined silicon. Micro-machining has been used in this case to produce cm-scale

components with μm-scale precision. In contrast to all previous vacuum tunneling devices, the relative position of the electrodes is controlled through use of electrostatic forces applied between the elements. The electrostatic forces induce deflection of a micro-machined silicon cantilever spring. Replacement of the piezoelectric actuator with an electrostatic actuator is important for the following reasons. First, the electrostatic actuator is insensitive to thermal drifts and immune to the problems of creep associated with piezoelectric actuators. Also the response of the electrostatic actuator is a function only of the geometry and mechanical properties of the device, whereas the response of the piezoelectric actuator is also dependent on the characteristics of the piezoelectric material, which may not be reproducible between devices or over time. Finally, the electrostatic actuator may be miniaturized more easily because the scaling laws are known exactly, and the fabrication is less complex than for the piezoelectric actuator. The device described here can be modified for incorporation into a wide variety of sensors. Monolithic devices including sensor and control electronics are also feasible.

The tunnel sensor described here consists of three components which are constructed from 200 μm silicon wafers. The wafers have been polished on both surfaces and are coated with >0.5 μm SiO_2 which is patterned by standard photo-lithographic techniques. The wafers are etched in Ethylene Diamine Pyrocatechol (EDP), removing the parts of the silicon wafers not covered by the SiO_2 mask. After etching, the remaining oxide is removed in a buffered HF etch. A new oxide layer >1 μm thick is then grown on all surfaces of the structure. Gold electrodes are thermally evaporated onto the components the sensor through shadow masks which have been fabricated by the same micro-machining techniques. The SiO_2 serves as a dielectric isolation layer between the metal films and the silicon substrate. Figure 1 shows a sketch of the components which result from etching and metallization. The components are approximately 4 cm^2 in area. The inner rectangular area of the folded cantilever spring can be deflected upward or downward relative to the outer segments by application of an electric potential between the large electrode and a corresponding deflection counter-electrode which is deposited on another component of the sensor. Given the mechanical properties of the silicon as well as the dimensions of the spring structure, we can calculate the properties of the spring. Because the spring constant scales rapidly with the dimensions of the legs, its characteristics can easily be tailored to meet the needs of a specific application.

Various methods for manufacturing a suitable tunneling tip are available.[7,10] Recently, we have developed the following procedure for micro-machining a silicon tip directly from the silicon substrate. An oxide-coated surface of the silicon is first patterned by photo-lithography to leave only a 60 μm x 60 μm square of oxide. When etched in EDP, the edges of the oxide are undercut. When the undercutting is complete, the square fragment of oxide is carried away, leaving a pyramid-shaped silicon tip. A scanning electron microscope micrograph of a typical tip is shown in Fig. 1. The active surfaces of the tips are prepared by evaporation of 3000 Å thick Au films through a shadow mask. The tunnel sensor is then assembled as shown in Fig. 2.

Once assembled, a bias voltage is applied to the electrostatic deflection electrodes to close the electrodes and establish a tunnel current. Active regulation of the tip-electrode separation using feedback control of the tunneling current is carried out as for STM. The tunnel position sensor implemented in this way is generally applicable to a wide range of sensing applications. The properties of a tunnel sensor applied to measurements of acceleration are described below. Operation of the device as an accelerometer may be achieved in either of two ways. In each case, acceleration is measured by sensing the deflection of the spring-supported silicon mass.

In the first approach, denoted as open loop, acceleration is measured at frequencies above the feedback loop bandwidth. When the sensor is subjected to an acceleration, ∂a, the deflection of the folded cantilever spring, ∂z, is given by $\partial z = \partial a / (\omega_0^2 - \omega^2)$[11], where $\omega_0 = \sqrt{k/m}$ is the resonant frequency of the spring supported mass.[12] Since the current varies as $\partial I = - I \alpha \sqrt{\Phi}\, \partial z$, the responsivity is given by :

$$\frac{\partial I}{\partial a} = - \frac{I \alpha \sqrt{\Phi}}{(\omega_0^2 - \omega^2)} . \qquad (2)$$

If the noise in the device is dominated by shot noise in the tunnel current, $I_n = \sqrt{2\, e\, I}$, the noise-equivalent acceleration (NEa) is given by :

$$NEa = \frac{I_n}{\partial I / \partial a} = \frac{(\omega_0^2 - \omega^2)}{\alpha} \sqrt{\frac{2\, e}{I\, \Phi}} . \qquad (3)$$

The noise-equivalent acceleration is defined as the minimum acceleration that could be detected in a 1 Hz bandwidth.

As shown in (2), the responsivity in the open loop method varies as $\sqrt{\Phi}$, which may depend on operating conditions. Variations in $\sqrt{\Phi}$ or other parameters which effect

the dependence of the tunnel current on electrode separation may be corrected for by adding a small modulation to the actuator voltage and measuring the resulting modulation in the tunnel current at that frequency. The ratio of the amplitudes of modulation directly yields the sensor sensitivity. This simple in-situ calibration may be performed continuously during operation of the sensor for applications which require high absolute accuracy.

In the second approach, denoted as closed loop, acceleration is measured for all frequencies less than the feedback loop bandwidth. In this case, the feedback loop responds to an acceleration by adjusting the force applied by the actuator so as to prevent any changes in the relative displacement of the tunneling electrodes. In this approach, the variations in the voltage applied to the actuator become the signal. For the electrostatic actuator in the present device, the force required to maintain constant electrode separation is given by :

$$F = m a = \frac{\varepsilon A V^2}{2 d^2} , \tag{4}$$

where A is the area of the deflection electrodes and d is the separation between the electrodes. The responsivity is then given by

$$\frac{\partial V}{\partial a} = \frac{m d^2}{\varepsilon A V} . \tag{5}$$

An advantage of this closed-loop approach is that the responsivity (5) is now independent of the height of the tunnel barrier or other properties of the tunnel electrodes as opposed to case for the open-loop approach. Shot noise in the tunnel current at frequencies within the bandwidth of the feedback loop causes fluctuations in the deflection voltage. These variations in deflection voltage produce changes in tunnel electrode separation, and therefore, variations in tunnel current which cancel the shot noise. The amplitude of the shot noise-induced voltage fluctuations is given by :

$$V_n = \sqrt{\frac{2 e}{I \Phi}} \frac{k \varepsilon A V}{m^2 d^2} . \tag{6}$$

The noise equivalent acceleration sensitivity is obtained by dividing the responsivity (5) by the noise (6) and is exactly the same as the open loop sensitivity (3).

The sources of noise observed in vacuum tunneling devices are not fully understood. At high frequency, shot noise and Johnson noise are expected to dominate. At lower frequencies, noise with a 1/f characteristic typically dominates. This noise may originate from slow drifts in the device structure, or environmental sources of noise, such as vibration, or air currents. Thermal drift, which leads to differential thermal expansion may also contribute to the low frequency noise in vacuum tunneling devices. Other

mechanisms for 1/f noise have been proposed.[13,14] With the replacement of the piezoelectric actuator by an electrostatic actuator, the problems associated with hysteresis, creep and thermal drift in piezoelectric materials should be greatly reduced. Contributions to the noise in tunneling due to fluctuations in the momentum transported have been considered.[15,16] This source of noise is not expected to be significant in our measurements.

The ultimate sensitivity of the tunnel sensor is limited by the noise characteristics of the vacuum tunnel junction. With the feedback loop closed and constant electrode separation being maintained, the tunnel current noise spectrum can be measured. Typical spectra for a current of 1.3 nA and bias of 100 mV are shown in Fig. 3 for different settings of the bandwidth of the feedback circuit. For this current, shot noise should contribute 2×10^{-14} A/$\sqrt{\text{Hz}}$, which is below the observed noise. The current noise due to the components of the electrical feedback circuit is also well below the observed noise. The tunnel current noise power spectrum varies approximately as 1/f for frequencies below 10^3 Hz. This result is consistent with noise measurements reported elsewhere,[17] and is likely due to environmental noise sources such as vibrations or thermal drifts. At frequencies greater than 10^4 Hz, an electrical resonance related to the deflection electrodes introduces additional noise.

By applying a low-frequency modulation to the tunnel current set-point in the feedback circuit, a modulation in the deflection voltage and tunnel current are produced. The barrier height, Φ, may be determined from the ratio of the amplitudes of the modulations. For the Au electrodes in this device, measurements of Φ have given a value of 0.5 eV. With $\Phi = 0.5$ eV, the data in Fig. 4 implies that the measured sensitivity to variations in the tip-sample separation is 3×10^{-4} Å/$\sqrt{\text{Hz}}$ at a frequency of 1 kHz. Given a cantilever mass of 30 mg and a measured spring constant of 60 N/m as well as the dependence of the tunnel current upon separation, the responsivity of the sensor to changes in acceleration may be calculated. Below the resonant frequency of about 200 Hz, the responsivity is 3×10^{-4} A/g. With the observed noise of the sensor, this corresponds to a sensitivity of 1×10^{-8} g/$\sqrt{\text{Hz}}$ at 10 Hz. At 1 kHz, the sensitivity is 1×10^{-7} g/$\sqrt{\text{Hz}}$. In each case, the measured noise included contributions from accelerations in the laboratory, so the actual sensitivity is probably somewhat better.

achieved. This would allow low-cost production of sensors of this type as transducers for application to a wide variety of measurement needs. In particular, miniature pressure sensors and microphones could be constructed with tunnel sensor technology. The use of a tunnel sensor as the transducer in a pneumatic infrared detector is currently being explored.[18]

The research described in this paper was performed by the Center for Space Microelectronics Technology, Jet Propulsion Laboratory, California Institute of Technology, and was jointly sponsored by the Defense Advanced Research Projects Agency and the National Aeronautics and Space Administration, Office of Aeronautics, Exploration and Technology.

For comparison, the sensitivity of a capacitive displacement transducer may be calculated. It is assumed that the electrode separation is no less than 1/100 of the electrode length, that the voltage is no greater than the limit for dielectric breakdown in vacuum, and that sensitivity is limited by the shot noise at the ac measurement frequency. With these assumptions, the capacitive transducer has a theoretically-limited sensitivity to variations in electrode separation of approximately 0.2 $\text{Å}/\sqrt{\text{Hz}}$. In this limit, the theoretical capacitive transducer is more than 3 orders of magnitude less sensitive than the existing tunneling transducer, and more than 4 orders of magnitude less sensitive than the theoretical limit to the tunneling transducer.

Since all of the components of the tunnel sensor can be prepared using standard lithographic techniques, miniaturization over several orders of magnitude can be readily

[1] F. Rudolf, Sensors and Actuators 4, 191 (1983).
[2] K.E. Petersen, A. Shartel and N. Raley, IEEE Trans. Electron Devices ED-29, 23 (1982).
[3] C.S. Sander, J.W. Knutti, and J.D. Meindl, IEEE Trans. Electron Devices ED-27, 927 (1980).
[4] E. Stemme and G. Stemme, IEEE Trans. Elect. Dev. 37, 648 (1990).
[5] D.L. Gardner, T. Hofler, S.R. Baker, R.K. Yarber and S.L. Garrett, J. Lightwave Tech. LT-5, 953 (1987).
[6] H.V. Allen, S.C Terry and D.W. De Bruin, Sensors and Actuators 20, 153 (1989).
[7] G. Binnig and H. Rohrer, IBM J. Res. Develop. 30, 355 (1986).
[8] S.B. Waltman, W.J. Kaiser, Sensors and Actuators 19, 201 (1989).
[9] K.E. Petersen, Proc. IEEE 70, 420 (1982).
[10] R.B. Marcus et al. Appl. Phys. Lett. 56, 236 (1990).
[11] In the low-frequency limit, this reduces to $\partial z = (m/k)\,\partial a$, which is Hooke's Law. Damping has been ignored in this discussion.
[12] It is assumed that the surface of the tunnel counter-electrode is flat and therefore ds = dz. If the surface of the counter-electrode is rough, ds = dz/cos(Q), where Q is the angle between the normal to the surface and the z axis.
[13] M.E. Welland and R.H. Koch. Appl. Phys. Lett. 48, 724 (1986).
[14] J.B. Pendry, P.D. Kirkman and E. Castano, Phys. Rev. Lett. 57, 2983 (1986).
[15] M.F. Bocko, K.A. Stephensen, and R.H. Koch, Phys. Rev. Lett. 61, 726 (1988).
[16] B. Yurke and G.P. Kochanski, Phys. Rev. B to be published (1990).
[17] D.W. Abraham, C.C. Williams, and H.K. Wickramasinghe, Appl. Phys. Lett. 53, 1503 (1988).
[18] T.W. Kenny, S.B. Waltman, J.K. Reynolds, and W.J. Kaiser to be published.

FIGURE CAPTIONS

Figure 1. A drawing of the components of the tunnel sensor is shown. The folded cantilever spring with integral tip is shown on the lower right. It is manufactured by patterning both surfaces of the silicon wafer and etching until the tunnel tip had formed. The components which support the tunneling counter-electrode and the deflection counter-electrode are shown on the left and are manufactured by patterning only one surface of the wafer. Au films are deposited through micro-machined shadow masks to form the deflection and tunneling electrodes. The tabs with the square holes allow the components to be constrained laterally by alignment pins.

Figure 2. A SEM micrograph of a typical micro-machined silicon tip. The tip has been coated by 3000 Å of Au.

Figure 3. An exploded view of the assembled tunnel sensor showing the orientations of the components. From top to bottom are the deflection counter-electrode, the tunneling counter-electrode, and the folded cantilever spring. The shaded regions on the spring correspond to the Au films which are deposited through shadow masks.

Figure 4. This figure is a plot of the spectrum of the measured noise in the tunnel current at a bias of 100 mV and current of 1.3 nA while operating in air. The bandwidth of the feedback circuit was deliberately adjusted to be less than 0.1 Hz for the data shown as circles. For the data plotted as squares, the bandwidth was set at the maximum value that did not produce oscillations, which was 200 Hz for this device. A resonance in the electrostatic deflection system contributes to the noise at frequencies above 5 kHz.

FIGURE 1

ORIGINAL PAGE
BLACK AND WHITE PHOTOGRAPH

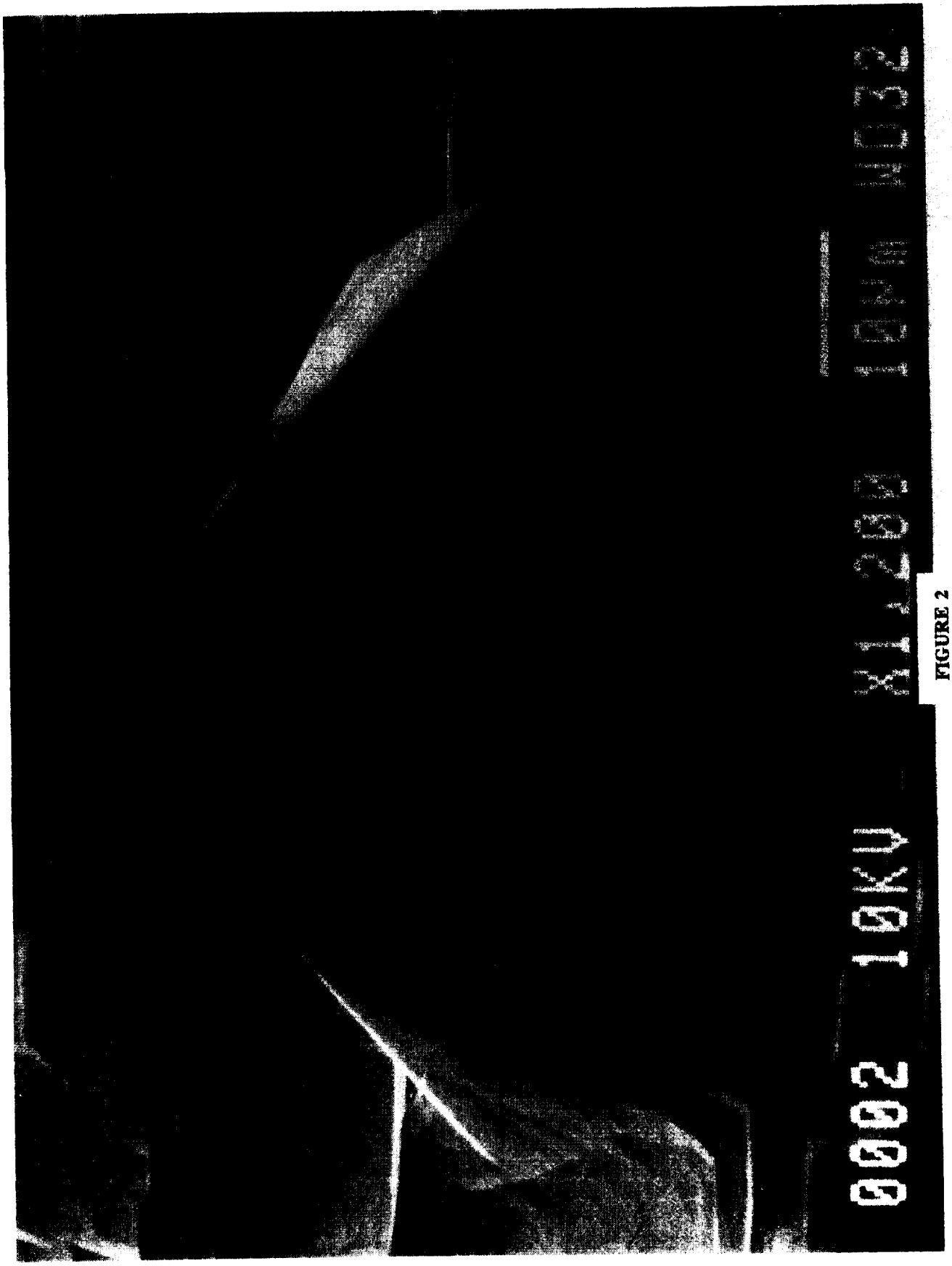

FIGURE 2

FIGURE 3

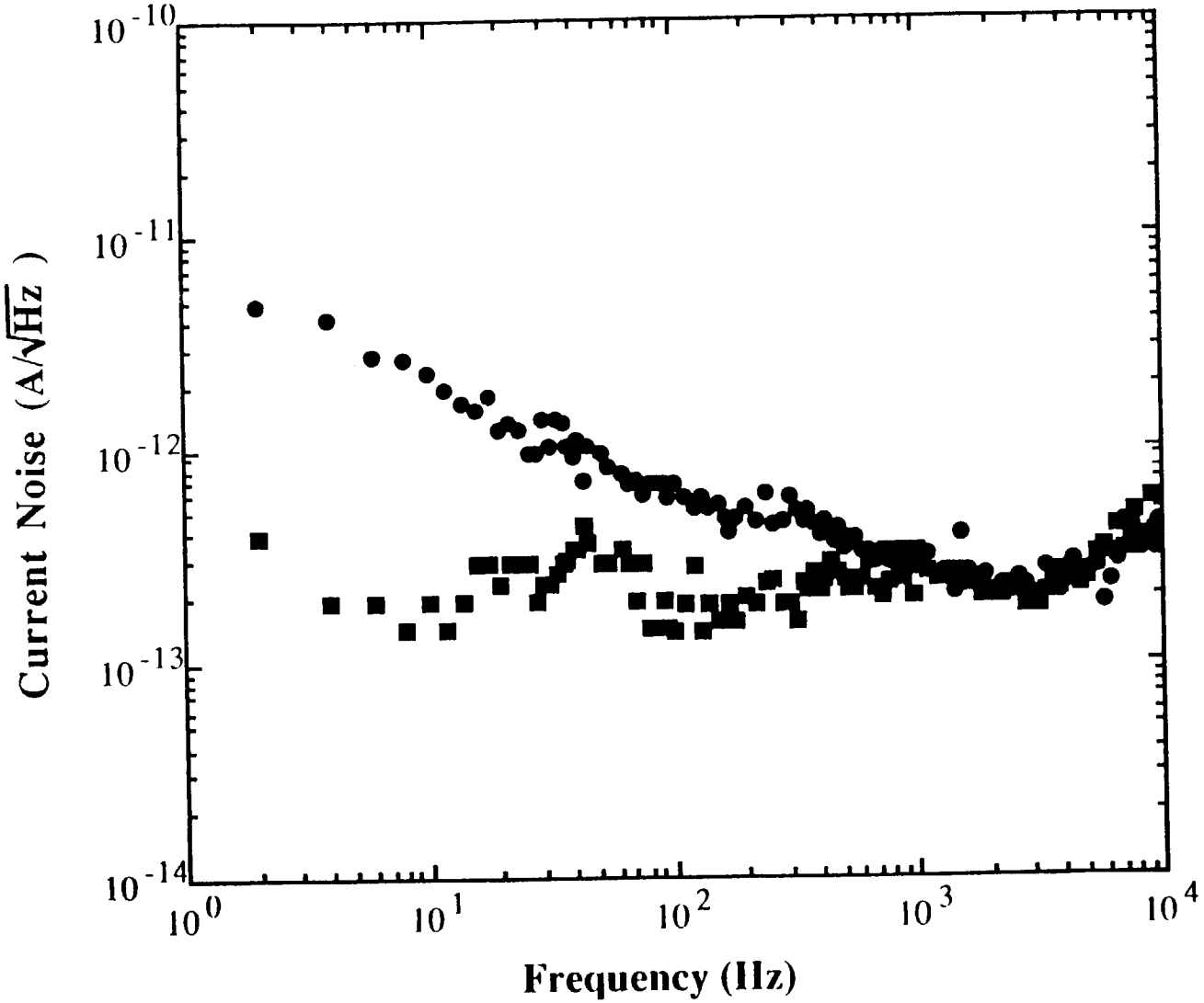
Current Noise (A/√Hz)
10^-10
10^-11
10^-12
10^-13
10^-14
10^0
10^1
10^2
10^3
10^4
Frequency (Hz)

FIGURE 4